NUMERICAL ANALYSIS OF HEAT TRANSFER ENHANCEMENT WITH THE USE OF γ-AL₂O₃/WATER NANOFLUID AND LONGITUDINAL RIBS IN A CURVED DUCT

by

Hosseinali SOLTANIPOUR [a*], Parisa CHOUPANI [b], and Iraj MIRZAEE [c]

[a] Department of Mechanical Engineering, Urmia University of Technology, Urmia, Iran
[b] Department of Mechanical Engineering, University of Tabriz, Tabriz, Iran
[c] Department of Mechanical Engineering, Urmia University, Urmia, Iran

This paper presents a numerical investigation of heat transfer augmentation using internal longitudinal ribs and γ-Al₂O₃/water nanofluid in a stationary curved square duct. The flow is assumed 3-D, steady, laminar, and incompressible with constant properties. Computations have been done by solving Navier-Stokes and energy equations utilizing finite volume method. Water has been selected as the base fluid and thermo-physical properties of γ-Al₂O₃/water nanofluid have been calculated using available correlations in the literature. The effects of Dean number, rib size and particle volume fraction on the heat transfer coefficient and pressure drop have been examined. Results show that nanoparticles can increase the heat transfer coefficient considerably. For any fixed Dean number, relative heat transfer rate (The ratio of the heat transfer coefficient in the case of γ-Al₂O₃/water nanofluid to the base fluid) increases as the particle volume fraction increases; however, the addition of nanoparticle to the base fluid is more useful for low Dean numbers. In the case of water flow, results indicate that the ratio of heat transfer rate of ribbed duct to smooth duct is nearly independent of Dean number. Noticeable heat transfer enhancement, compared to water flow in smooth duct, can be achieved when γ-Al₂O₃/water nanofluid is used as the working fluid in ribbed duct.

Key words: *curved duct, Dean number, laminar flow, heat transfer enhancement, particle volume fraction*

Introduction

The subject of heat transfer augmentation is of significant interest in developing high-performance thermal systems. Generally, convective heat transfer can be increased passively by different methods such as changing the flow geometry or improving the effective thermal behaviors of the working fluid. The first approach deals with structuring the flow and temperature fields by geometrical modifications using roughness elements, ribs, turbulators, or vortex generators. In the case of heat transfer in the curved ducts, which is the main subject of this paper, some researchers investigated the rib or fin effects on heat transfer augmentation.

---

* Corrresponding author; e-mail: h.soltanipour@gmail.com

Numerical study of [1] showed that, the rib-induced heat transfer augmentation is attributed to the promotion of secondary vortex motion. Chang et al. [2] showed that, augmented Nusselt numbers in the static rib-roughened curved duct fall in the range of 1.21-1.45 times of smooth-wall duct. Papadopoulos et al. [3] studied the laminar incompressible developing flow in a curved square duct with four longitudinal fins. They found that fin height plays an important role on heat transfer enhancement. In the curved pipes, the numerical results of [4] showed that presence of internal fins causes the secondary flows to separate into small regions among the fins and more vortices are generated relative to the finless. They obtained an optimum fin height about 0.8 of pipe radius for Dean numbers less than 100.

In the second approach, various techniques have been proposed to enhance the heat transfer performance of working fluids. In fact, conventional heat transfer fluids, including oil, water, and ethylene glycol mixture are poor heat transfer fluids; considering this fact, numerous methods have been taken to improve the thermal conductivity of these fluids by suspending nano-sized particle materials in liquids. Choi et al. [5] showed that by adding a small amount (less than 1% by volume) of nanoparticles into the conventional liquids, the thermal conductivity of the fluid increases up to approximately two times. Several researches [6-9] stated that with low concentration of nanoparticles (1-5 vol.%), the thermal conductivity of the suspensions can be increased more than 20%. Heris et al. [10] performed laminar convective heat transfer experiments on CuO/water and Al_2O_3/water nanofluids and concluded that the heat transfer enhancement by nanofluids depends on several factors, including nanoparticle type, size, base fluid temperature, flow regime, and the boundary conditions. Nguyen et al. [11] experimentally investigated the heat transfer characteristics of Al_2O_3/water nanofluids for an electronic cooling application. They found that with 6.8% particle volume concentration, the heat transfer coefficient is increased as much as 40% compared to the base fluid. From the numerical viewpoint, Akbarinia et al. [12] presented a study of nanofluids under mixed laminar convection in a curved tube. They compared the variations of Nusselt number with Grashof number for various volume percentages of Al_2O_3 nanoparticles in water. They found that for large Grashof number the skin friction reduces. Wen et al. [13] studied Al_2O_3/water nanofluid heat transfer for laminar flow under constant wall heat flux boundary condition, and reported that the heat transfer coefficient increases with increasing the Reynolds number and nanoparticle concentration, particularly at the entrance region. They expressed that thermal developing length for nanofluid was greater than the base fluid. Heris et al. [14] presented a solution for enhancement of laminar forced convection with a nanofluid flowing in a tube under constant wall temperature boundary condition using the homogeneous model. They assumed that the flow and energy equations of the base fluid are not affected by the presence of the suspended particles. Recently, experimental investigations of [15] showed heat transfer enhancement capabilities of coolants with suspended nanoparticles (Al_2O_3 dispersed in water) for radial flow in cooling device. For steady, laminar radial flow of a nanofluid between a heated disk and a flat plate with axial coolant injection, the results showed that the Nusselt number increases with particle volume fraction and Reynolds number, and decreases by increasing disk spacing.

This paper investigates the heat transfer enhancement using γ-Al_2O_3/ water nanofluid flow in a curved square duct with internal longitudinal ribs. The effects of three important parameters, including Dean number, the rib size, and the particle volume fraction of on the heat transfer coefficient and pressure drop is presented in the following sections.

Statement of the problem

The problem under investigation is a 3-D steady, forced laminar convection flow of γ-Al$_2$O$_3$/ water nanofluid flowing inside a stationary curved duct having the side length and curvature radius of a and R, respectively. The geometry of the duct is shown in fig. 1. According to the figure, the Cartesian co-ordinate system is used for flow analysis, which its origin is taken at the center O of the curved duct. An internal rib with square cross-section area is mounted at the midway of the heated wall. Heat is transferred only through the outer wall of the duct, and is transported by water (base fluid) or γ-Al$_2$O$_3$/water nanofluid with different volume fractions.
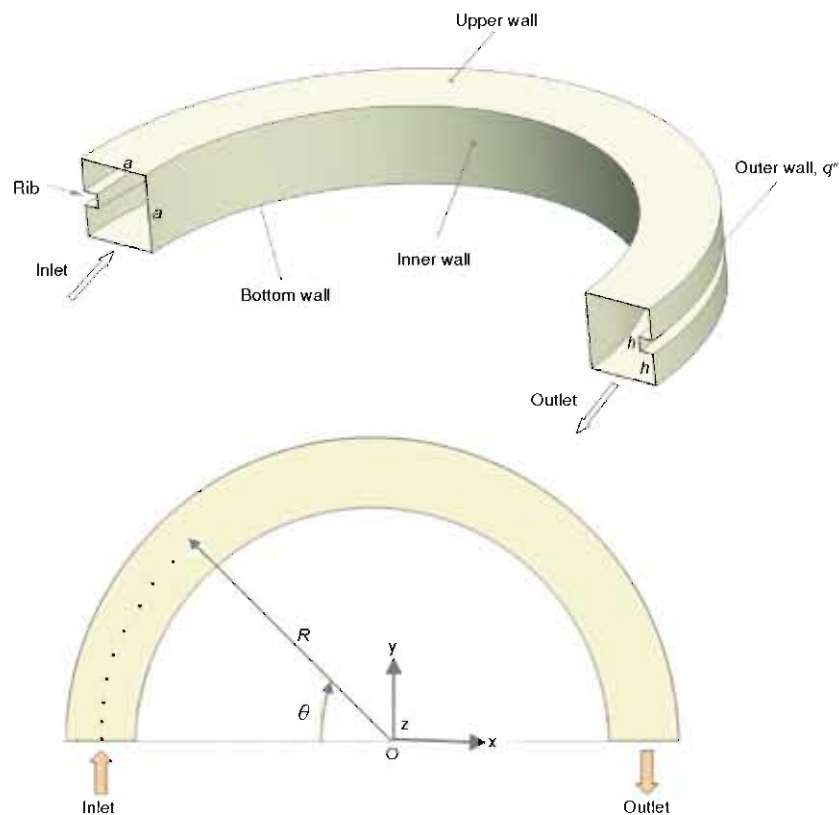

Figure 1. Geometry of ribbed curved duct and co-ordinate system

The Reynolds, Dean, and Nusselt numbers for the current problem are defined as follows:

$$\mathrm{Re} = \frac{V_{in} D_h}{\nu} \tag{1}$$

$$\mathrm{De} = \mathrm{Re}\sqrt{\frac{D_h}{R}} \tag{2}$$

$$\mathrm{Nu} = \frac{\bar{h} D_h}{k} \tag{3}$$

where V_{in} and D_h are the average inlet velocity and the hydraulic diameter of curved duct, respectively. In the cases with rib, three different values of rib size, *i. e.*, h/a = 1/10, 1/7, and 1/5 is considered to investigate the rib size on heat transfer enhancement.

Governing equations and boundary conditions

Most of the nanoparticles used in heat transfer applications, have extremely small dimensions (finer than 40 nm); so it has been suggested that these particles may be easily fluidized and consequently, considered as a conventional single-phase fluid. Therefore, the effective thermophysical properties of nanofluids can be expressed as a function of the properties of both constituents and their respective concentrations [16, 17]. Thus, governing equations as known for single-phase fluids can be employed for nanofluids. Under such conditions, and assuming 3-D, steady, laminar, incompressible flow with constant fluid properties and negligible viscous dissipation in the energy equation, the general conservation equations in the vectorial form can be written as:

– continuity equation

$$\mathrm{div}(\rho \vec{V}) = 0 \tag{4}$$

– momentum equation

$$\mathrm{div}(\rho \vec{V}\vec{V}) = -\vec{\nabla}P + \mu \nabla^2 \vec{V} \tag{5}$$

– energy equation

$$\mathrm{div}(\rho \vec{V} C_p T) = \mathrm{div}(k\vec{\nabla}T) \tag{6}$$

where $\vec{V}$ is the velocity vector and P – the static pressure. All fluid properties are evaluated at the reference temperature that is the fluid inlet temperature T_{in}.

The governing equations of the fluid flow are non-linear and partial differential equations, subjected to the following boundary conditions. At the duct inlet section, uniform axial velocity (V_{in}) and temperature (T_{in}) are specified. At the outlet section, atmospheric pressure boundary condition is adopted. On the walls of the duct and rib surfaces, the no-slip boundary condition prevails. The constant heat flux is specified only on the outer wall, whereas other walls of the curved duct are assumed to be adiabatic.

The average local convective heat transfer coefficient $h(\theta)$ is defined by:

$$h(\theta) = \frac{q''}{T_w(\theta) - T_m(\theta)} \tag{7}$$

where $T_w(\theta)$ is the average local temperature of the outer wall and $T_m(\theta)$ – the local bulk fluid temperature which given by:

$$T_m(\theta) = \frac{\int \rho C_p U T \mathrm{d}A}{\int \rho C_p U \mathrm{d}A} \tag{8}$$

where U is the axial velocity and A – the cross-sectional area perpendicular to the axial direction.

And finally, the average heat transfer coefficient on the outer wall, $\bar{h}$ can be computed as

$$\bar{h} = \frac{1}{A_{ow}} \int h(\theta)\mathrm{d}A_{ow} \tag{9}$$

Thermophysical properties of the γ-Al$_2$O$_3$ nanofluid

Assuming that the γ-Al$_2$O$_3$ nanoparticles are dispersed uniformly within water and form a homogeneous mixture, knowing the properties of the constituents, and their respective concentrations, the effective properties of γ-Al$_2$O$_3$/water nanofluid can be evaluated using some classical formulas as well-known for two-phase fluids. In the following equations, the subscripts p', bf and nf refer to the particles, the base-fluid and the nanofluid, respectively:

$$\rho_{nf} = (1 - \phi)\rho_{bf} + \phi\rho_p \tag{10}$$

$$(C_P)_{nf} = (1 - \phi)(C_P)_{bf} + \phi(C_P)_p \tag{11}$$

$$\mu_{nf} = \mu_{bf}(123\phi^2 + 73\phi + 1) \tag{12}$$

$$k_{nf} = k_{bf}(4.97\phi^2 + 2.72\phi + 1) \tag{13}$$

Equations (10) and (11) are general relationships used to compute the density and specific heat for a classical two- phase mixture [17], while eq. (12) has been obtained by performing a least-square curve fitting of some scarce experimental data available for the mixtures considered [6, 7, 18].

In recent years, many research groups focused on theoretical prediction and experimental determination of nanofluids thermophysical properties. According to the literature review, one can conclude that even for the same nanofluids, different research groups reported inconsistent correlations for the effective thermal conductivity and viscosity of nanofluids [19-22]. So, further research is needed to identify the accurate correlations for nanofluids properties. Despite probable errors in the viscosity and thermal conductivity given by eqs. (12) and (13), these correlations have been adopted in this study because of their simplicity.

Numerical method and grid system

Computational fluid dynamics (CFD) was used for solving this problem. The system of governing eqs. (4-6) were solved by control volume approach. Control-volume technique converts the governing equations to a set of algebraic equations that can be solved numerically. The control volume approach employs the conservation statement or physical law represented by the entire governing equations over finite control volumes. First order upwind scheme was employed to discretize the convection terms, while the central differencing scheme was used for diffusion terms. Pressure and velocity were coupled using SIMPLE algorithm [23]. Linear systems resulting from discretization schemes were solved using Gauss-Seidel linear equation solver. For all simulations performed in the present study, converged solutions were considered when the residuals resulting from iterative process for all governing equations were lower than 10^{-7}.

In order to ensure grid independency, three grid sizes were submitted to an extensive testing of results. Comparison of different grid system results (for the average heat transfer coefficient and pressure drop in the case De = 2000 and h/a = 1/5) is shown in tab. 1. It is observed that the grid system 50 × 50 × 100 (50 × 50 on the cross-sectional plane and 100 nodes along the axial direction) has satisfactory independency with respect to the number of elements used. Consequently, aforementioned grid was adopted for different geometries and flow conditions.

Table 1. The grid independency study

Grid size	$\dfrac{\bar{h}_{rd}}{\bar{h}_{sd}}$	$\dfrac{\Delta P_{rd}}{\Delta P_{sd}}$
40 × 40 × 50	1.20	1.58
50 × 50 × 100	1.35	1.53
60 × 60 × 120	1.36	1.51

Validation of the present simulation

There exists, to our knowledge, no experimental result regarding the case of the flow and heat transfer of nanofluids in a curved duct. Therefore, in order to validate the computer model, we have had to compare our numerical results with available data obtained for conventional fluids. To examine the accuracy of present results, we first compared numerical results with experimental data of [24]. The comparison is illustrated in fig. 2, wherein the variation of axial velocity at two cross-sectional planes (i. e., θ = 36 and 90°) for water flow inside a curved duct as a function of distance along the radial location (at z = 0) is presented. As shown in fig. 2, the calculated distributions of axial velocity demonstrate good agreement with the measured results.
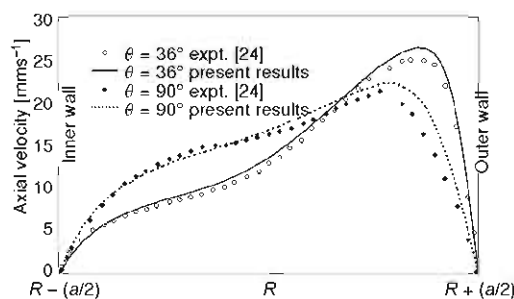

Figure 2. Axial velocity as a function of the radial location in the midplane of the cross-section for De = 226
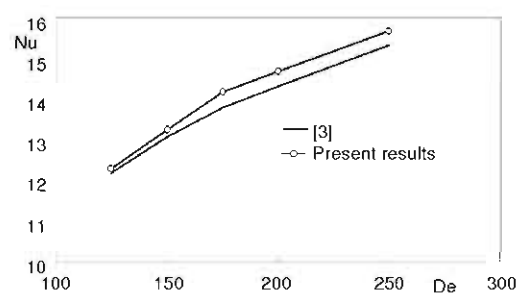

Figure 3. Comparison of results from present work with Papadopoulos et al. [3]

Another comparison was made with numerical results from [3] for water flow through a curved duct for isothermal boundary condition. The average Nusselt number vs. Dean number is depicted in fig. 3. It is observed that the maximum deviation of 2.75% appears for the Nusselt number in the case of De = 175.

Results and discussions

In order to analyze the effects of the ribs and γ-Al_2O_3/water nanofluid on improving thermal performance of a curved duct, the computations were carried out for four cases:
(1) smooth curved duct with water as the working fluid,
(2) smooth curved duct with γ-Al_2O_3/water nanofluid as the working fluid,
(3) ribbed curved duct with water as the working fluid, and
(4) ribbed curved duct with γ-Al_2O_3/water nanofluid as the working fluid.
For the four above mentioned cases, the Dean number varies from 500-2000.

The effects of rib size on heat transfer and pressure drop

To understand the mechanism of heat transfer enhancement using longitudinal ribs in a curved duct, velocity vectors at two cross-sectional planes (i. e., θ = 45° and θ = 135°) for

three cases (smooth curved duct, and ribbed curved ducts with rib size $h/a = 1/10$ and 1/5 at De = 500), are shown in fig. 4. For smooth curved duct (no rib case), as water enters the duct, due to curvature, the centrifugal force affects the flow field and a pair of counter rotating vortices generated. Furthermore, as fluid moves downstream, a small pair of vortices is formed near the outer wall (at $\theta = 135°$). In the ribbed case, with rib size $h/a = 1/10$, the presence of rib causes to form an additional pair of vortices near the outer wall at $\theta = 45°$. When fluid develops to $\theta = 135°$, the vortices formed near rib sides, move toward the center of cross section, whereas vortices near the inner wall remain unchanged. When rib size increases, the vortex structure becomes complicated. A comparison of velocity vectors at $\theta = 45°$ between the ribbed cases $h/a = 1/10$ and $h/a = 1/5$, indicates that, as the rib size increases, the vortices formed near the outer wall become stronger. The comparison of velocity vectors for the ribbed cases reveals that the duct with higher rib

Figure 4. Velocity vectors on two cross-sectional planes. On each cross-sectional plane, outer wall is at right-hand side

size, has an additional pair of vortices near rib sides at $\theta = 135°$, and totally there are three pairs of counter rotating vortices. Finally, one can see the effect of ribs on formation and development of secondary motion and their abilities in intensifying the vortices, which is beneficial for heat transfer applications.

Now the effects of rib size on heat transfer enhancement and pressure drop are presented in details. In this regard, three cases with rib sizes $h/a = 1/10$, $h/a = 1/7$, and $h/a = 1/5$ for Dean numbers 500, 1000, 1500, and 2000 have been investigated. The followings discuss the average heat transfer coefficient on the outer heated wall, $\bar{h}$ and pressure losses, ΔP (pressure difference between inlet and outlet). It should be mentioned that in the following, subscript sd refers to smooth curved duct, while subscript rd is related to the curved duct with a rib mounted on heated wall. Figure 5 shows that the using rib has, in fact, produced a considerable improvement of the heat transfer on the duct wall. Thus, for the particular values of De = 1500 and $h/a =$ 1/5, for example, the ratio of convective heat transfer coefficient in the ribbed curved duct to-smooth curved duct (which is defined as $\bar{h}_{rd}/\bar{h}_{sd}$) is approximately 1.42, that is to say, the heat transfer coefficient has increased by 42% over that of the smooth curved duct. It is clear that for any fixed Dean number, the duct of rib size $h/a = 1/5$ has the higher ratio of the convective heat transfer coefficient compared to the other ones. It should be pointed out that for smooth and ribbed curved ducts, by increasing Dean number, the heat transfer coefficient in-
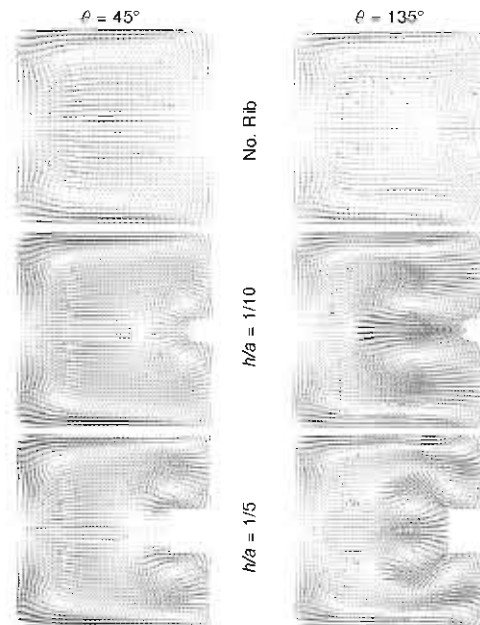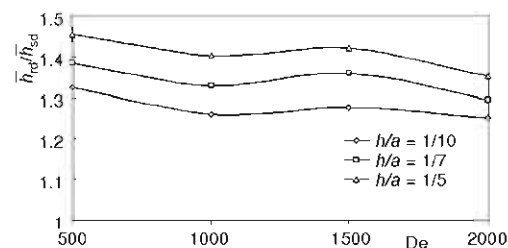

Figure 5. The effect of rib size on the convective heat transfer coefficient for different Dean numbers for the base fluid

476

Soltanipour, H., *et al.*: Numerical Analysis of Heat Transfer Enhancement with ...
THERMAL SCIENCE: Year 2012, Vol. 16, No. 2, pp. 469-480

creases because of the promotion of secondary vortex motion, while fig. 5 indicates that for any fixed rib size, the ratio of the convective heat transfer coefficient is nearly independent of Dean number. In fact, the maximum variation of $\bar{h}_{rd}/\bar{h}_{sd}$ is related for the case $h/a = 1/5$ is 0.1; therefore, one can conclude that this ratio is approximately constant for Dean numbers considered here. Finally, the maximum heat transfer enhancement is about 45%, which is related to $h/a = 1/5$ and De = 500.
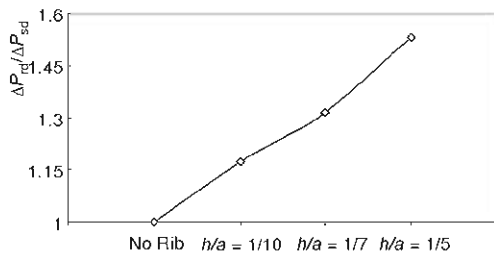
Figure 6. The effect of rib size on the pressure drop for base fluid

The effects of rib on flow losses are presented in fig. 6. The pressure drop ratio of ribbed curved duct to- smooth curved duct (which is defined as $\Delta P_{rd}/\Delta P_{sd}$) raises with increasing the rib size. Such an increase is related to increase of solid surfaces, which causes to growth of shear stresses. For example, the pressure drop for rib $h/a = 1/7$, has increased by 32% over that of the smooth curved duct. It is interesting to mention that for Dean numbers considered here, although the increase of Dean number in smooth and ribbed ducts, leads to higher pressure drop, but the pressure drop ratio is nearly independent of Dean numbers. In other words, for a fixed rib size, the pressure drop ratio of ribbed curved duct to- smooth curved duct is the same for any Dean number.

The effects of nanoparticles on heat transfer and pressure drop in smooth curved duct

Over the following, some significant results indicating the beneficial influence of addition of γ-Al_2O_3 nano-particles to the base fluid in the case of smooth curved duct, are presented and discussed. It is necessary to cite that in the following subscript nf implies nanofluid (mixture of water and γ-Al_2O_3), while subscript bf refers to the base fluid. In the present study, we are interested to establish on the average basis, the overall influence of nanoparticles on the heat transfer. Figure 7 shows the global effects of particle volume fraction, ϕ on the heat transfer enhancement for different Dean numbers. The averaged heat transfer coefficient for water γ-Al_2O_3 mixture is denoted by $\bar{h}_{nf}$. The heat transfer coefficient ratio, $\bar{h}_{nf}/\bar{h}_{bf}$ is particularly interesting since it indicates the degree of heat transfer enhancement compared to the base fluid. One can clearly observe from fig. 7 that, $\bar{h}_{nf}/\bar{h}_{bf}$ increases considerably with the augmentation of
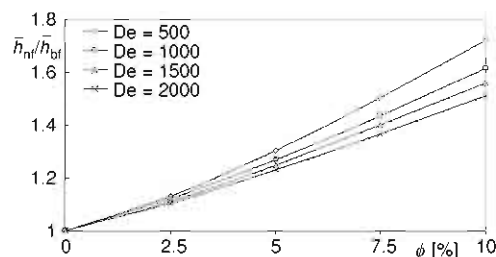
Figure 7. The effect of the particle volume fraction on the heat transfer coefficient in smooth curved duct

particle loading parameter, ϕ and decreases with increasing Dean number. Thus, for De = 500, $\bar{h}_{nf}/\bar{h}_{bf}$ has values 1.15, 1.30, 1.50, and 1.72 for $\phi = 2.5$, 5, 7.5, and 10%, respectively, that is to say that the averaged heat transfer coefficient has increased by 15, 30, 50, and 72%, with respect to that of the base fluid (water). These results have obviously indicated the beneficial effects due to the nanoparticles, effects that may be explained by the fact that with the presence of such particles; the thermal properties of the resulting mixture are improved con-

siderably. For a particular value of $\phi = 10\%$, for example, it has been found that the values of the product ρC_p and the thermal conductivity, k have increased as much as 18.4% and 32%, respectively, with respect to those corresponding to the case $\phi = 0$. For higher Dean number, $h_{nf}/\bar{h}_{bf}$ although being always greater than 1, it being less important. On the other hand, for fixed value of ϕ, say $\phi = 10\%$, for example, this ratio has as values, 1.51, 1.56, 1.62, and 1.72 for De = 2000, 1500, 1000, and 500, respectively. Finally, for the ranges of the governing parameters studied in this study and considering the values of $\bar{h}_{nf}/\bar{h}_{bf}$, one may say that the maximum heat transfer enhancement for smooth curved duct is about 72% which is related to De = 500 and $\phi = 10\%$.

Figure 8 shows the pressure drop ratio of the nanofluid-to-base fluid for various particle concentrations. In general, one can observe, $\Delta P_{nf}/ /\Delta P_{bf}$ increases considerably with the particle volume fraction. For the specific value $\phi = 7.5\%$, for example, $\Delta P_{nf}/\Delta P_{bf}$ has a value of 4.10, i. e., the pressure drop is nearly quadruple of that corresponding to the base fluid given identical operating conditions. In fact, for water γ-Al$_2$O$_3$ nanofluid in particular, its effective dynamic viscosity is almost multiplied by a factor of 2.24 for the case $\phi = 7.5\%$ with respect to that of the base fluid (i. e. $\phi = 0$). It is very interesting to note that,

Figure 8. The effect of the particle volume fraction on the pressure drop in smooth curved duct

numerical results show for a given value of ϕ, the value of $\Delta P_{nf}/\Delta P_{bf}$ is nearly identical to any Dean number. Finally, for the range of the particle volume fraction considered here, the maximum pressure drop ratio reaches to 6.8, which belongs to $\phi = 10\%$.
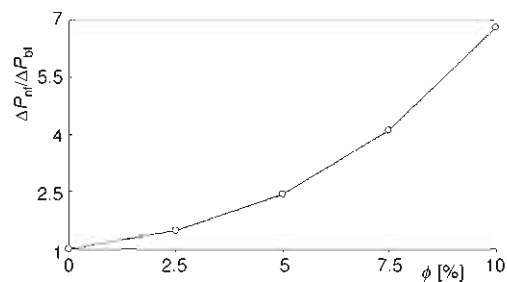
The effects of ribs and nanoparticles on flow parameters

To gain a better understanding of heat transfer augmentation using γ-Al$_2$O$_3$/ water nanofluid and longitudinal ribs, the convective heat transfer coefficient for nanofluid flow in ribbed curved duct has been compared with water flow in smooth duct at the same conditions. It is necessary to say that subscript nfr denotes nanofluid flow in the ribbed duct, while subscript bfs is related to base fluid flow in smooth curved duct. Relative heat transfer coefficient versus particle volume fraction for different Dean numbers are depicted in figs. 9, 10, and 11 for $h/a = $ = 1/10, 1/7, and 1/5, respectively. For three rib sizes considered here, relative heat transfer coefficient curves have the similar trend. For any fixed Dean number, relative heat transfer coefficient increases linearly with the augmentation of particle volume fraction. Moreover, for specified value of ϕ, h_{nfr}/h_{bfs}, is higher for low Dean numbers. This result is similar to nanofluid flow in a smooth curved duct. The results of ribbed ducts exhibited that mounting a longitudinal rib with size $h/a = 1/5$ on the heated wall, can increase the heat transfer coefficient up to 45% relative to smooth duct (for De = 500 for water
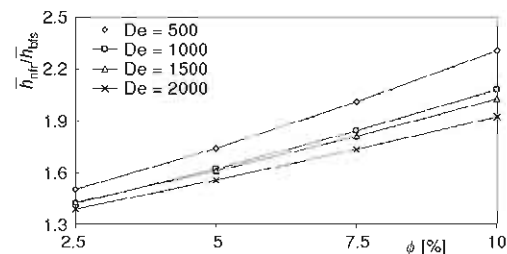
Figure 9. The effect of the particle volume fraction on the heat transfer coefficient in ribbed curved duct for rib size $h/a = 1/10$
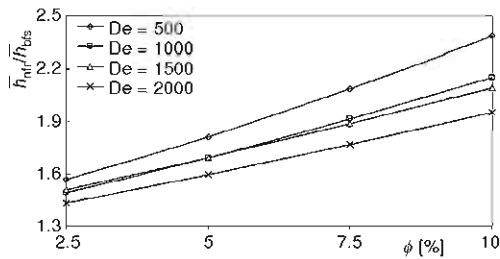
478

Soltanipour, H., *et al.*: Numerical Analysis of Heat Transfer Enhancement with ...
THERMAL SCIENCE: Year 2012, Vol. 16, No. 2, pp. 469-480

Figure 10. The effect of the particle volume fraction on the heat transfer coefficient in ribbed curved duct for rib size $h/a = 1/7$

as working fluid), and by γ-Al$_2$O$_3$/water nanofluid with $\phi = 10\%$ instead of water, heat transfer can be enhanced 72% in a smooth curved (for De = 500). As shown in fig. 11, for instance, the heat transfer coefficient in ribbed curved duct with rib size $h/a = 1/5$ and γ-Al$_2$O$_3$/water nanofluid with $\phi = 10\%$ as the working fluid, is 2.5 times that of corresponding to the base fluid in smooth curved duct for De = = 500. Such an increase in the heat transfer coefficient, in fact, reveals the combined effects of two passively heat transfer enhancement methods. For the smallest rib size (*i. e. $h/a = 1/10$*), fig. 9 indicates that, augmented heat transfer coefficients for γ-Al$_2$O$_3$/water nanofluid with particle volume fraction ranging 2.5-10 (for De = 500), fall in the range of 1.5-2.3 times of water flow in smooth-wall duct. Consequently, heat transfer rate in a curved duct can be augmented remarkably; this requires geometrical modifications (mounting rib) and improving thermal behaviors of coolant fluid (by adding of nanoparticles to the base fluid).
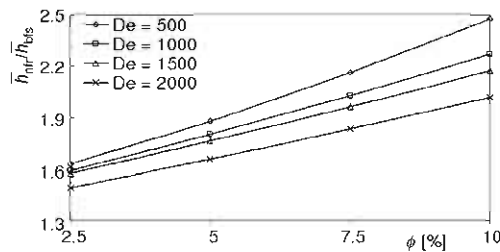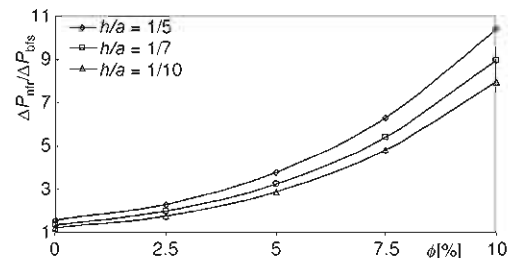

Figure 11. The effect of the particle volume fraction on the heat transfer coefficient in ribbed curved duct for rib size $h/a = 1/5$

Figure 12. The effect of the particle volume fraction on the pressure drop in ribbed curved duct

Despite the use of nanofluids has beneficial heat transfer enhancement capabilities, it is to be expected that, because of their increased viscosity, they also increase pressure losses. Figure 12 illustrates the dependence of the pressure drop ratio of nanofluid flow in ribbed curved duct to-base fluid flow in the smooth curved duct, with respect to the particle loading parameter ϕ for various rib sizes. As shown in the figure, the pressure drop increases considerably by increasing the particle volume fraction or rib size. For example, for a 7.5% particle fraction of γ-Al$_2$O$_3$/water nanofluid, the pressure drop ratio, has the values, 4.81, 5.40, and 6.29 for $h/a = = 1/10, 1/7$, and $1/5$, respectively.

Although, the use of γ-Al$_2$O$_3$/water nanofluid with higher particle volume fractions and larger rib sizes has the considerable heat transfer rate, it remains to be seen what practical limits of particle volume fraction and rib size could be used in various applications. Therefore, the benefits of the higher heat transfer rate versus the corresponding severe increase in flow losses should be considered.

Conclusions

In this paper, forced laminar flow of γ-Al_2O_3/water nanofluid and heat transfer behaviors in a ribbed curved duct have been investigated using control volume method. Results have been presented for a range of Dean number ($500 \leq De \leq 200$), three rib sizes ($h/a = 1/10$, 1/7, and 1/5) and particle volume fraction ranging 0-10%. In the case of water flow in ribbed duct, significant heat transfer enhancement (relative to smooth duct) is achieved without a large pressure-drop penalty. For γ-Al_2O_3/ water nanofluid flow in smooth curved duct (for $De = 500$ and $\phi = 10\%$), the maximum heat transfer coefficient is approximately 1.72 times of water flow and corresponding pressure drop ratio is 6.8. In a ribbed curved (with rib size $h/a = 1/5$ and γ-Al_2O_3/ water nanofluid with $\phi = 10\%$) as working fluid, the heat transfer coefficient increased as much as 150% compared to the base fluid in smooth curved duct. Despite the increase of the heat transfer coefficient is desired, increase of this parameter is influenced by adverse effect of dramatic pressure drop caused by increased viscosity of working fluid and solid surfaces of the duct.

Nomenclature

C_p — specific heat at constant pressure, [$Jkg^{-1}K^{-1}$]
D_h — hydraulic diameter (= $4A/p$), [m]
h — rib height, [m]
k — thermal conductivity, [$Wm^{-1}K^{-1}$]
T — temperature, [K]
U — axial/streamwise velocity, [ms^{-1}]

Greek symbols

μ — dynamic viscosity, [Nm^2s^{-1}]

ρ — density, [kgm^{-3}]
ϕ — volume fraction, [–]

Subscripts

bf — base fluid
in — conditions at the duct inlet
ow — outer wall
w — wall

References

[1] Ko, T. H., Numerical Investigation on Laminar Forced Convection and Entropy Generation in a Curved Rectangular Duct with Longitudinal Ribs Mounted on the Heated Wall, *International Journal of Thermal Science, 45* (2006), 4, pp. 390-404
[2] Chang, S. W., Lin, C. C., Liou, J. S., Heat Transfer in a Reciprocating Curved Square Duct Fitted with Longitudinal Ribs, *International Journal of Thermal Sciences, 47* (2008), 1, pp. 52-67
[3] Papadopoulos, P. K., Hatzikonstantinou, P. M., Thermally Developing Flow in Curved Square Ducts with Internal Fins, *Heat and Mass Transfer, 42* (2005), 1, pp. 30-38
[4] Nobari, M. R. H., Gharali, K., A Numerical Study of Flow and Heat Transfer in Internally Finned Rotating Straight Pipes and Stationary Curved Pipes, *International Journal of Heat and Mass Transfer, 49* (2006), 5-6, pp. 1185-1194
[5] Choi, S. U. S., *et al.*, Anomalously Thermal Conductivity Enhancement in Nanotube Suspensions, *Applied Physics Letters, 79* (2001), 14, pp. 2252-2254
[6] Masuda, H., *et al.*, Alteration of Thermal Conductivity and Viscosity of Liquid by Dispersing Ultra-Fine Particles (Dispersion of γ-Al_2O_3, SiO_2, and TiO_2 Ultra-Fine Particles), *Netsu Bussei, 7* (1993), 4, pp. 227-233
[7] Lee, S., *et al.*, Measuring Thermal Conductivity of Fluids Containing Oxide Nanoparticles, *Journal of Heat Transfer, Transactions of ASME 121* (1999), 2, pp. 280-289
[8] Xuan, Y., Li, Q., Heat Transfer Enhancement of Nanofluids, *International Journal of Heat and Fluid Flow, 21* (2000), 1, pp. 58-64

[9] Xuan,Y., Roetzel, W., Conceptions for Heat Transfer Correlation of Nanofluids, *International Journal of Heat and Mass Transfer, 43* (2000), 19, pp. 3701-3707

[10] Heris, S. Z., Esfahany, M. N., Etemad, G., Investigation of CuO/Water Nanofluid Laminar Convective Heat Transfer through a Circular Tube, *Journal of Enhanced Heat Transfer, 13* (2006), 4, pp. 279-289

[11] Nguyen, C. T., *et al.*, Heat Transfer Enhancement Using Al$_2$O$_3$-water Nanofluid for an Electronic Liquid Cooling System, *Applied Thermal Engineering, 27* (2007), 8-9, pp. 1501-1506

[12] Akbarinia, A., Behzadmehr, A., Numerical Study of Laminar Mixed Convection of a Nanofluid in Horizontal Curved Tubes, *Applied Thermal Engineering, 27* (2007), 8-9, pp. 1327-1337

[13] Wen, D., Ding, Y., Experimental Investigation into Convective Heat Transfer of Nanofluids at the Entrance Region under Laminar Flow Conditions, *International Journal of Heat and Mass Transfer, 47* (2004), 24, pp. 5181-5188

[14] Heris, S. Z., Esfahany, M. N., Etemad, G., Numerical Investigation of Nanofluid Laminar Convection Heat Transfer through a Circular Tube, *Numerical Heat Transfer, 52* (2007), 11, A, pp. 1043-1058

[15] Gherasim, I., *et al.*, Experimental Investigation of Nanofluids in confined Laminar Radial Flows, *International Journal of Thermal Sciences, 48* (2009), 8, pp. 1486-1493

[16] Xuan,Y., Roetzel, W., Conceptions for Heat Transfer Correlation of Nanofluids, *International Journal of Heat and Mass Transfer, 43* (2000), 19, pp. 3701-3707

[17] Pak, B. C., Cho, Y. I., Hydrodynamic and Heat Transfer Study of Dispersed Fluids with Submicron Metallic Oxide Particles, *Experimental Heat Transfer, 11* (1998), 2, pp.151-170

[18] Wang, X., Xu, X., Choi, S. U. S., Thermal Conductivity of Nanoparticles-Fluid Mixture, *Journal of Thermophysics and Heat Transfer, 13* (1999), 17, pp. 474-480

[19] Murshed, S. M. S., Leong, K. C., Yang, C., Thermophysical and Electrokinetic Properties of Nanofluids – A Critical Review, *Applied Thermal Engineering, 28* (2008), 17-18, pp. 2109-2125

[20] Kakac, S., Pramuanjaroenkij, A., Review of Convective Heat Transfer Enhancement with Nanofluids, *International Journal of Heat and Mass Transfer, 52* (2009), 13-14, pp. 3187-3196

[21] Wang, X. Q., Mujumdar, A. S., Heat Transfer Characteristics of Nanofluids: A Review, *International Journal of Thermal Sciences, 46* (2007), 1, pp. 1-19

[22] Murugesan, C., Sivan, S., Limits for Thermal Conductivity of Nanofluids, *Thermal Science, 14* (2010), 1, pp. 65-71

[23] Patankar, S. V., Numerical Heat Transfer and Fluid Flow, Hemisphere Publishing Corporation, New York, USA, 1980

[24] Hille, P., Vehrenkamp, R., Schulz-Bubois, E. O., The Development and Structure of Primary and Secondary Flow in a Curved Square Duct, *Journal of Fluid Mechanics, 151* (1985), pp. 219-241